Proceedings of ICFD 10:
Tenth International Congress of Fluid Dynamics
December 16-19, 2010, Stella Di Mare Sea Club Hotel, Ain Soukhna, Red Sea, Egypt

ICFD10-EG-3018

Non-Darcy Effects on Conjugate Natural Convection in Saturated Porous Layer Sandwiched by Finite Thickness Walls

Al-Farhany , K.
School of Mechanical, Aerospace and Civil Engineering, The University of Manchester, P.O. Box 88, Manchester M60 1QD, UK
Khaled.AlFarhany@postgrad.manchester.ac.uk

Turan, A.
School of Mechanical, Aerospace and Civil Engineering, The University of Manchester, P.O. Box 88, Manchester M60 1QD, UK
A.Turan@manchester.ac.uk

ABSTRACT

Unsteady conjugate natural convective heat transfer in a two-dimensional variable porosity layer sandwiched between two walls has been studied numerically. The Generalization model has been used to solve the governing equations in the saturated porous region. The Boussinesq approximation assumed to be valid. The vertical walls are impermeable and subjected to a horizontal gradient of temperature while the horizontal walls are adiabatic. A finite volume approach has been used to solve the dimensionless governing equations and the pressure velocity coupling is treated with the SIMPLE algorithm. The model has been validated with available experimental, analytical/computational studies. A correlation to evaluate the average Nusselt number has been proposed as a function of Rayleigh number, Darcy number, including a number of physical geometrical and material property ratios.

KEYWORDS: Heat transfer, natural convection, porous media, non-Darcy, Conjugate, CFD and finite volume.

INTRODUCTION

An equally large body of research has emerged with respect to investigations of convective heat and mass transfer in rectangular porous cavities and vertical surfaces with uniform/non-uniform heat flux and surface temperatures. The classical Darcy formulation has been used as well as the Darcy-Brinkman model, the Darcy-Forscheimmer model and Darcy-Brinkman-Forscheimmer model. These areas have been thoroughly reviewed recently by Nield and Bejan [1].

Sen [2] considered the Darcy-Brinkman convective flow in a shallow porous rectangular cavity with adiabatic upper and lower plate boundaries and differentially heated sidewalls. An important non-Darcian study also has been presented by Lauriat and Prasad [3] for a heated vertical porous cavity. The inertia and viscous forces on natural convection is examined via the Darcy-Brinkman-Forchheimer. Nithiarasu [4] studied the effect of the differences in existing porous medium flow models on flow and heat transfer in the context of heat flux boundary condition. The results showed that the effects of non-linear drag term and porosity are significant at higher Rayleigh and Darcy numbers. Numerical investigation for transient free convection in a two-dimensional square cavity filled with a porous medium conducted by Saeid and Pop [5]. These results are in good agreement with the results obtained by Walker and Homsy [6], Bejan [7], Weber [8], Gross et al [9] and Manole and Lage [10], Bankvall [11] .Also, the results show that the time required to get to steady state is shorter for the high Rayleigh number and longer for low Rayleigh number.

In the last three decades, a wide range of studies have been published in the literature emphasizing the conjugate heat transfer phenomena in a porous media. It is of practical importance in for example, high performance insulation for buildings and cold storage installations. Nield and Bejan [1] presented many reviews of the existing studies on such topics. In addition to Ingham and Pop [12,13], Pop and Ingham [14], Vafai [15] and Al Amiri [16] studies.

Numerical investigations for non-Darcian effects on transient conjugate natural convection-conduction heat transfer from a two-dimensional vertical plate fin embedded in a high-porosity medium were carried out by Hung et al [17]. The results have shown that the inertial effects on heat transfer characteristic are negligible at earlier times. On the other hand the effect becomes increasingly important at longer times. Furthermore, as mentioned above, two-dimensional transient conjugate free convection due to a vertical plate in a porous medium was investigated both analytically and numerically by Vynnycky and Kimura [18] and Kimura et al [19].

Important contributions were also made by Saeid [20] regarding the steady conjugate natural convection–conduction heat transfer in a two-dimensional vertical porous enclosure. The wall with a finite thickness was heated horizontally, while the outer surfaces of the vertical walls were isothermal at different temperatures, as opposed to the horizontal boundaries that were kept insulated. The Darcy model was considered in this model and the finite volume method was used to solve the dimensionless governing equations. The results indicate that in both the wall and the porous layer, the heat is transferred mainly by conduction and the average Nusselt number is approximately constant. Earlier Al-Amiri et al [21] studied numerically two-dimensional steady state conjugate natural convection in a fluid saturated porous cavity bounded by a conducting vertical wall. The results showed that as the wall thickness increases, the overall Nusselt number is reduced, while the average Nusselt number increases when the Rayleigh number increases. These results are in good agreement with the results obtained by Kaminski and Prakash [22], Hribersek and Kuhn [23], Wansophark et al [24], Al-Amiri [25].

In this paper, unsteady conjugate natural convective heat transfer in a two-dimensional porous layer sandwiched between two walls is investigated. The horizontal boundaries of the cavity are adiabatic and the vertical walls are maintained at fixed different temperatures. The generalized model with the Boussinesq approximation is used to solve the governing equations in the saturated porous region and the conductivity equation has been used to solve the energy equation in the finite thickness wall layer. A finite volume approach has been used to solve the dimensionless governing equations and the pressure velocity coupling is treated with the SIMPLE algorithm in the porous media domain. The results are presented in streamline, isothermal and Nusselt number profiles.

METHODOLOGY

The model is constructed by using a two-dimensional porous cavity sandwiched between two finite thickness walls filled with an isotropic porous medium as shown in Figure (1). The horizontal boundaries of the cavity are adiabatic and the vertical walls are maintained at fixed different temperatures T_h and T_c. The Brinkman-Forchheimer-extended Darcy (generalization) model has been used to solve the governing equations. Isotropic, homogeneous, local thermal balance, and saturated with an incompressible fluid has been assumed. All the properties have been assumed to be constant except the density. The flow is driven by a buoyancy fource due to temperature variations. The density variations are described by the Boussinesq approximation:

$$\rho = \rho\left[1-\beta_T (T - T_o)\right] \tag{1}$$

Where $\beta_T = -\frac{1}{\rho}\left(\frac{\partial \rho}{\partial T}\right)_{P,C}$ is the thermal expansion coefficient.

The two-dimensional continuity, energy, momentum in the x and y directions for unsteady natural convection (properly non-dimensionalised) are given as in Nithiarasu et al [26]:

Continuity equation is:

$$\frac{\partial U}{\partial X} + \frac{\partial V}{\partial Y} = 0 \tag{2}$$

X-momentum equation is:

$$\frac{1}{\varepsilon}\frac{\partial U}{\partial \tau} + \frac{1}{\varepsilon^2}U\cdot\frac{\partial U}{\partial X} + \frac{1}{\varepsilon^2}V\cdot\frac{\partial U}{\partial Y} = -\frac{\partial P}{\partial X} - \frac{\Pr}{Da}\cdot U - \frac{1.75}{\sqrt{150}}\cdot\frac{\sqrt{U^2+V^2}}{\sqrt{Da}}\cdot\frac{U}{\varepsilon^{3/2}} + \frac{Pr}{\varepsilon}\left(\frac{\partial^2 U}{\partial X^2} + \frac{\partial^2 U}{\partial Y^2}\right) \tag{3}$$

Y-momentum equation is:

$$\frac{1}{\varepsilon}\frac{\partial V}{\partial \tau} + \frac{1}{\varepsilon^2}U\cdot\frac{\partial V}{\partial X} + \frac{1}{\varepsilon^2}V\cdot\frac{\partial V}{\partial Y} = -\frac{\partial P}{\partial Y} - \frac{Pr}{Da}\cdot V - \frac{1.75}{\sqrt{150}}\cdot\frac{\sqrt{U^2+V^2}}{\sqrt{Da}}\cdot\frac{V}{\varepsilon^{3/2}} + \frac{Pr}{\varepsilon}\left(\frac{\partial^2 V}{\partial X^2} + \frac{\partial^2 V}{\partial Y^2}\right) + Ra\cdot Pr\cdot T \tag{4}$$

Energy equation is:

$$\sigma\cdot\frac{\partial T}{\partial \tau} + U\cdot\frac{\partial T}{\partial X} + V\cdot\frac{\partial T}{\partial Y} = \frac{\partial^2 T}{\partial X^2} + \frac{\partial^2 T}{\partial Y^2} \tag{5}$$

and the energy equation for the walls is:

$$\frac{1}{\Gamma}\cdot\frac{\partial T_W}{\partial \tau} = \frac{\partial^2 T_W}{\partial X^2} + \frac{\partial^2 T_W}{\partial Y^2} \tag{6}$$

The heat flux and the temperatures at the solid-porous media interface must be the continuous.

$$-k_w\frac{\partial T_w}{\partial X} = -k_{eff}\frac{\partial T}{\partial X} \tag{7}$$

where the subscript p and w refer to the porous and the wall respectively.

Also, the heat transfer at the walls are defined as the following:

$$Nu = \frac{1}{A}\int_0^A -\frac{\partial T}{\partial X}\cdot\partial Y \tag{8}$$

where Nu is the average Nusselt number,

The non-dimensional parameters are:

$$X = \frac{x}{L},\ Y = \frac{y}{L},\ A = \frac{H}{L},\ D = \frac{d}{L},\ U = \frac{uL}{\alpha}, V = \frac{vL}{\alpha},\ Pr = \frac{\nu}{\alpha}$$

$$T = \frac{\bar{T} - \bar{T}_c}{\bar{T}_h - \bar{T}_c},\quad \alpha = \frac{k_{eff}}{\left(\rho\cdot c_p\right)_f},\quad P = \frac{pL^2}{\rho\alpha^2},\ Ra = \frac{g\beta_T \Delta T L^3}{\nu\alpha},$$

$$\tau = \frac{t\alpha}{L^2},\ k_r = \frac{k_w}{k_f},\ \Gamma = \frac{k_w/\left(\rho\cdot c_p\right)_w}{k_{eff}/\left(\rho\cdot c_p\right)_f},\ k_{eff} = \varepsilon k_f + (1-\varepsilon)k_s$$

$$\sigma = \frac{\varepsilon\left(\rho\cdot c_p\right)_f + (1-\varepsilon)\left(\rho\cdot c_p\right)_s}{\left(\rho\cdot c_p\right)_f},\ Da = \frac{K}{L^2},\ Pr = \frac{\nu}{\alpha} \tag{9}$$

The equations (2)-(8) are solved by using the non-dimensional initial boundary conditions:

$U,V = 0$ *at* $X = 0,1$, *at any* Y : $U,V = 0$ *at* $Y = 0, A$, *at any* X

$T_h = 1$ *at* $X = -D$, *at any* Y : $T_c = 0$ *at* $X = 1 + D$, *at any* Y

$$\frac{\partial T}{\partial Y} = 0 \text{ at } Y = 0,\ A \text{ at any } X : Nu = \frac{1}{A}\int_0^A -\frac{\partial T}{\partial X}\Bigg)_{x=-D,0,1,1+D} \cdot \partial Y$$

NUMERICAL METHOD

A finite volume approach has been used to solve the dimensionless governing equations (2)-(7). The transport process and the corresponding equations are strongly coupled, since the conjugate effect (convection-conduction) between the walls and the porous media. The primary steps for the pressure velocity coupling are treated using the SIMPLE algorithm tailored for the porous media domain by Patankar [27] and will not be presented here. A second order central discretization scheme is used for the momentum, energy equations, and the semi-implicit first order scheme is used for time step advancement in the momentum equations and the ADI method is adopted for the energy, John and Anderson [28]. The inertial term in momentum equations is considered a source term. In the porous media, different mesh sizes were tested and a 81*81 grid is adopted as reasonable for the low Rayleigh number while a 121*121grid was deemed adequate for the high Rayleigh number. The steady state was considered to have been arrived at when the changes in U, V, P and T satisfy the equation:

$$\frac{\sum_i \sum_j \left|\theta_{i,j}^{n+1} - \theta_{i,j}^{n}\right|}{\sum_i \sum_j \left|\theta_{i,j}^{n+1}\right|} \le 1*10^{-6} \qquad (10)$$

An in-house code developed for this study was validated using previous studies. For pure heat transfer in porous cavity without wall thickness, tables 1-4 show that the present results are in good agreement for most of the cases using various the Darcy, Darcy-Brinkman, Darcy-Forchhemier and generalized models.

As another check on the accuracy of the in-house code, the effect of the finite walls thickness has been compared with that of Saeid [20]. A heat transfer cases were run by using the Darcy model for different wall thermal conductivity ratios and wall thickness to cavity length. Figure (2) shows that the isotherms and streamlines of the present study are matched fairly well to Saeid predictions. Also, the average Nusselt numbers of the wall-porous media interface are in good agreement with Saeid. The results presented here are in good accord with the available experimental, analytical and numerical/computational studies.

RESULTS

In this section, the results are presented in streamline, isothermal and Nusselt numbers profiles. A correlation equation was provided to calculate the average Nusselt number on the internal left wall of the porous cavity as a function of different values of the non-dimensionless governing parameters, including the modified Rayleigh number ($100 \le Ra^* \le 1000$), Darcy Number ($10^{-4} \le Da \le 10^{-7}$), thermal conductivity ratio ($0.1 \le Kr \le 10$) and the ratio of wall thickness to its height ($0.1 \le D \le 0.4$). Where the modified Rayleigh number equal to the $Ra^* = Ra.\ Da$.

1.1 Wall thickness effects

To show the effects of the wall thickness (D), streamline and isotherms line are presented in Figure (3) for $Da=10^{-6}$, $Ra=1*10^{9}$, Pr=1.0, Kr=1 and different wall thickness. The circulation strength of the fluid in the porous medium is lower with thick walls as shown in Figure (3) (a) - (c). Also the isothermal lines shows that the most of the temperature variation still in the wall thickness due to conduction in the wall. These phenomena caused the decrease in heat transfer by convection in porous medium, because of the decreasing the temperature different. The average Nusselt numbers on the interface left wall porous decrease when the wall thickness is increased as shown in Figure (4). This means the heat transfer conduction are dominant in the porous cavity.

1.2 Thermal conductivity ratio effects

In Figure (3) (c) and (d) the streamlines, isotherms and iso-concentration are presented for $Da=10^{-6}$, Pr=1.0, $Ra=1*10^{9}$, D=0.4 and Kr= 1, 10 respectively to show the effect of the thermal conductivity ratio. It can be seen that, for the increase in the thermal conductivity ratio the circulation strength of the fluid in the porous cavity are increased. This is due to the thermal field in the porous cavity, as influenced by the increasing temperature gradients in the horizontal direction with increases in the thermal conductivity ratio. For $Da=10^{-6}$, $Ra=1*10^{9}$, Pr=1.0, D=0.1, the variation of the local Nusselt number on the vertical porous interface walls with thermal conductivity ratio are presented in figure (5). It show very clearly that the left and right local Nusselt numbers increases when the thermal conductivity increases along the high of the cavity. Also, it show that the heat flux on the hot left wall in equilibrium and equal to the heat flux on the cold right wall. These are happen because there is no heat generation assumed in the porous cavity and horizontal walls are insulated. For low thermal conductivity ratio there are no significant changes on the Nusselt number even with high Rayleigh number as shown in figure (6).

In general, the Nusselt number increases when the Rayleigh number increases as shown in figure (6).

1.3 Correlation equation for Nusselt number on the left porous interface wall

The correlation equations are most important for the engineering approximation equations for describe the dependent variable as a function of the independents variables

for all domain. The average Nusselt number on the interface left porous wall was correlated by

$$Nu = a * Da^{b} * Ra^{c} * D^{d} * Kr^{e} \quad (11)$$

Hundreds simulations were done to calculate the average Nusselt number on the internal left wall of the porous cavity. The non-dimensionless governing parameters were used for these simulations are: modified Rayleigh number ($100 \le Ra^{*} \le 1000$), Darcy Number ($10^{-4} \le Da \le 10^{-7}$), thermal conductivity ratio ($0.1 \le Kr \le 10$) and the ratio of wall thickness to its height ($0.1 \le D \le 0.4$). For the whole range of the parameters, the correlation equation is:

$$Nu = 0.0994 * Da^{0.3386} * Ra^{0.3385} * D^{-0.4188} * Kr^{0.5281} \quad (12)$$

CONCLUSIONS

Two-dimensional porous cavity sandwiched between two finite thickness walls filled with an isotropic porous medium has been investigated numerically by using a finite volume method. The results are presented in a porous medium for different values of the non-dimensionless governing parameters, including the modified Rayleigh number ($100 \le Ra^{*} \le 1000$), Darcy Number ($10^{-4} \le Da \le 10^{-7)}$, thermal conductivity ratio ($0.1 \le Kr \le 10$) and the ratio of wall thickness to its height ($0.1 \le D \le 0.4$. It show that as the wall thickness increases, the overall Nusselt number is reduced, while the average Nusselt number increases when the Rayleigh number and the thermal conductivity ratio increase. On the other hand, Nu increases when the Darcy number increases. A correlation to evaluate the average Nusselt numbers on the interface left wall is:

$$Nu = 0.0994 * Da^{0.3386} * Ra^{0.3385} * D^{-0.4188} * Kr^{0.5281}$$

REFERENCE

[1] D.A. Nield and A. Bejan, Convection in Porous Media, second ed.,Springer-Verlag, NY, 1995.

[2] A.K. Sen, Natural convection in a shallow porous cavity--the Brinkman model. International Journal of Heat and Mass Transfer, 1987. 30(5): p. 855-868.

[3] G Lauriat. and V. Prasad, Non-Darcian effects on natural convection in a vertical porous enclosure. International Journal of Heat and Mass Transfer, 1989. 32(11): p. 2135-2148.

[4] P. Nithiarasu, et al., Buoyancy driven flow in a non-Darcian, fluid-saturated porous enclosure subjected to uniform heat flux - A numerical study. Communications in Numerical Methods in Engineering, 1999. 15(11): p. 765-776.

[5] N.H. Saeid and I. Pop, Transient free convection in a square cavity filled with a porous medium. International Journal of Heat and Mass Transfer, 2004. 47(8-9): p. 1917-1924.

[6] K.L. Walker and G.M. Homsy, Convection in a porous cavity. Journal of Fluid Mechanics, 1978. 87(pt 3): p. 449-474.

[7] A. Bejan , On the boundary layer regime in a vertical enclosure filled with a porous medium. Letters in Heat and Mass Transfer, 1979. 6(2): p. 93-102.

[8] J.E. Weber, The boundary-layer regime for convection in a vertical porous layer. International Journal of Heat and Mass Transfer, 1975. 18(4): p. 569-573.

[9] R.J. Gross, M.R. Baer, and C.E. Hickox. Application of flux-corrected transport (fct) to high rayleigh number natural convection in a porous medium. in Heat Transfer, Proceedings of the International Heat Transfer Conference. 1986.

[10] .M. Manole and J.L. Lage. Numerical benchmark results for natural convection in a porous medium cavity. in American Society of Mechanical Engineers, Heat Transfer Division, (Publication) HTD. 1992.

[11] Bankvallc, Warme- und Stoffiibertragung, 1974. 7, 22.

[12] D.B. Ingham, I. Pop (Eds.), Transport Phenomenon in Porous Media, vol. I, Pergamon, Oxford, 1998.

[13] D.B. Ingham, I. Pop (Eds.), Transport Phenomena in Porous Media, vol. III, Elsevier, Oxford, 2005.

[14] I. Pop, D.B. Ingham, Convective Heat Transfer: Mathematical and Computational Modeling of Viscous Fluids and Porous Media, Pergamon, Oxford, 2001.

[15] K. Vafai, Handbook of Porous Media, second ed., Taylor and Francis Group, NY, 2005.

[16] A. Al-Amiri, Natural convection in porous enclosures: the application of the two-energy equation model, Numer. Heat Transfer: Part A 41(2002) 817–834.

[17] C.-I Hung, C.o.-K. Chen, and P. Cheng, Transient conjugate natural convection heat transfer along a vertical plate fin in a high-porosity medium. Numerical Heat Transfer; Part A: Applications, 1989. 15(1): 133-148.

[18] M.Vynnycky and S. Kimura, Transient conjugate free convection due to a vertical plate in a porous medium. International Journal of Heat and Mass Transfer, 1995. 38(2): p. 219-231.

[19] S. Kimura, et al., Conjugate natural convection in porous media. Advances in Water Resources, 1997. 20(2-3): p. 111-126

[20] N.H. Saeid, Conjugate natural convection in a vertical porous layer sandwiched by finite thickness walls. International Communications in Heat and Mass Transfer, 2007. 34(2): p. 210-216

[21] A. Al-Amiri, K. Khanafer, and I. Pop, Steady-state conjugate natural convection in a fluid-saturated porous cavity. International Journal of Heat and Mass Transfer, 2008. 51(17-18): p. 4260-4275

[22] D.A. Kaminski and C. Prakash, Conjugate natural convection in a square enclosure: effect of conduction in one of the vertical walls. International Journal of Heat and Mass Transfer, 1986. 29(12): p. 1979-1988.

[23] M. Hribersek and G. Kuhn, Conjugate heat transfer by boundary-domain integral method. Engineering Analysis with Boundary Elements, 2000. 24(4): p. 297-305.
[24] N. Wansophark, A. Malatip, and P. Dechaumphai, Streamline upwind finite element method for conjugate heat transfer problems. Acta Mechanica Sinica/Lixue Xuebao, 2005. 21(5): p. 436-443.
[25] A.M. Al-Amiri, Analysis of momentum and energy transfer in a lid-driven cavity filled with a porous medium. International Journal of Heat and Mass Transfer, 2000. 43(19): p. 3513-3527.
[26] P. Nithiarasu,, K.N. Seetharamu, and T. Sundararajan, Natural convective heat transfer in a fluid saturated variable porosity medium. International Journal of Heat and Mass Transfer, 1997. 40(16): p. 3955-3967.
[27] S.V. Patankar, Numerical Heat Transfer and Fluid Flow, Hemisphere Publishing Corporation, Washington, 1980.
[28] D. John and E.J. Anderson, Computational Fluid Dynamics: The Basics with Applications, ed. P. perback, Published 1995 by McGraw-Hill Higher Education, International edition. 1995.

NOMENCLATURE

A	aspect ratio
c_p	specific heat at constant pressure
d	thickness of the solid walls, m
D	non-dimensional wall thickness, m
Da	Darcy number,
g	gravitational acceleration, ms^{-2}
H	height of the cavity, m
K	permeability of the porous medium, m^2
k	thermal conductivity, $Wm^{-1} K^{-1}$
k_{eff}	effective thermal conductivity of porous medium, $m^{-1} K^{-1}$
k_f	thermal conductivity of the fluid, $Wm^{-1} K^{-1}$
k_w	thermal conductivity of the wall, $Wm^{-1} K^{-1}$
k_r	thermal conductivity ratio
L	length of the cavity, m
Nu	average Nusselt number
p	pressure, ms^{-2}
P	non-dimensional pressure
Pr	Prandtl number,
Ra	Rayleigh number for porous medium,
Ra^*	modified Rayleigh number for porous medium,
t	time, s
$\overline{T}$	dimensional temperature, K
T	non-dimensional temperature
u	velocity components in x-direction, ms^{-1}
U	non-dimensional velocity components in X-direction
v	velocity components in y-direction, $m\ s^{-1}$
V	non-dimensional velocity components in Y-direction
x	x coordinates, m
X	non-dimensional X-coordinates
y	y coordinates, m
Y	non-dimensional Y-coordinates

Greek symbols

α	effective thermal diffusivity , $m^2\ s^{-1}$
β_T	coefficient of thermal expansion , K^{-1}
Γ	is the wall to porous media heat capacity
ε	porosity of the porous media
ν	kinematic viscosity , $m^2\ s^{-1}$
θ	non-dimensional temperature
ρ	density, kgm^{-3}
τ	non-dimensional time

Subscripts

c	cold
h	hot
eff	effective
f	fluid
s	solid practical
w	wall

Table 1 Comparison of average Nusselt number at study stat with some previous results for Darcy model (pure heat transfer, N=0)

Author	*Nu*				
	Ra*=10	Ra*=50	Ra*=100	Ra*=500	Ra*=1000
Walker and Homsy [6]	1.38	1.98	3.091	8.40	12.49
Lauriat and Prasad [3]	1.07	---	3.09	----	13.41
Trevisan and Bejan [51]	---	2.02	3.27	---	18.38
Nithiarasu [43]	1.08	1.958	3.02	8.38	12.514
Present work	1.087	1.992	3.132	8.719	12.674

Table 2 Comparison of average Nusselt number at study stat with some previous results for Darcy-Brinkman model (N=0, Pr=1)

Author	*Nu*					
	$Da=10^{-6}$			$Da=10^{-2}$		
	Ra*=10	Ra*=100	Ra*=1000	Ra*=10	Ra*=100	Ra*=1000
Lauriat and Prasad [3]	1.07	3.06	13.2	1.02	1.70	4.26
Nithiarasu [43]	1.08	3.00	12.25	1.02	1.71	4.26
Present work	1.087	3.113	12.684	1.019	1.719	4.267

Table 3 Comparison of average Nusselt number at study stat with some previous results for Darcy- Forchhemeir model (N=0, Pr=1)

Author	*Nu*					
	$Da=10^{-6}$			$Da=10^{-2}$		
	Ra*=10	Ra*=100	Ra*=1000	Ra*=10	Ra*=100	Ra*=1000
Lauriat and Prasad [3]	1.07	2.97	9.62	1.06	2.28	5.55
Nithiarasu [43]	1.08	3.00	9.63	1.08	2.30	5.58
Present work	1.087	3.092	11.794	1.081	2.317	5.611

Table 4 Comparison of average Nusselt number at study state with some previous results for generalization model (N=0, Pr=1, Ra*=104)

Author	*Nu*	
	$Da=10^{-1}$	$Da=10^{-4}$
Lauriat and Prasad [3]	4.36	18.40
Beckerman [50]	4.39	20.59
Nithiarasu [43]	4.49	21.99
Present work	4.458	22.131

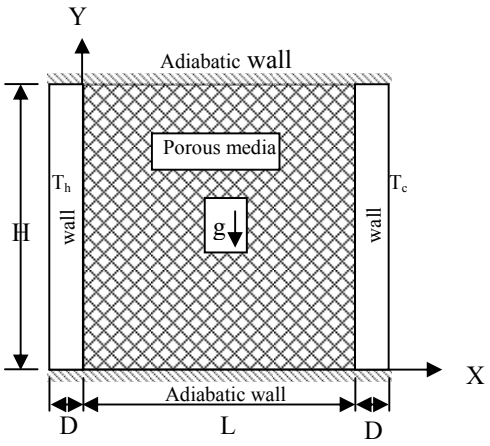

Figure (1) the geometry of the model

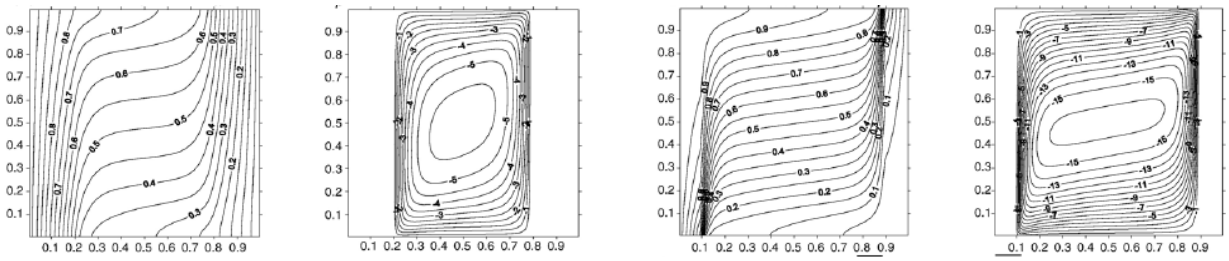

Saeid results (Nu_w=1.888 , Nu_P=1.888)

Saeid results (Nu_w=1.023 , Nu_P=10.238)

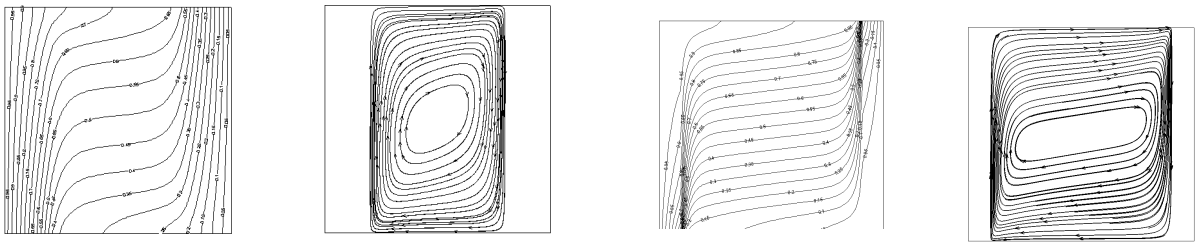

Present results (Nu_w=1.894 , Nu_P=1.893)

a

Present results (Nu_w=1.0251 , Nu_P=10.0250)

b

Figure (2) Comparison of present results with Saeid [20] results for Streamlines (right), isotherms (left) by using Darcy flow at Ra*=1000, a-(D=0.2, Kr=1), and b-(D=0.1, Kr=10).

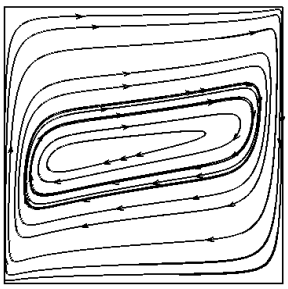

(a) Streamlines

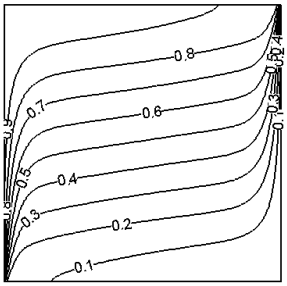

isotherms

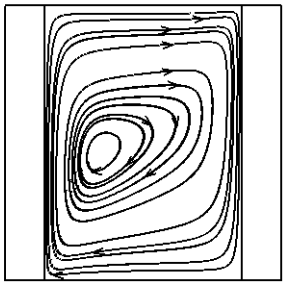

(b) Streamlines

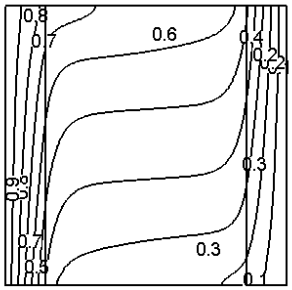

isotherms

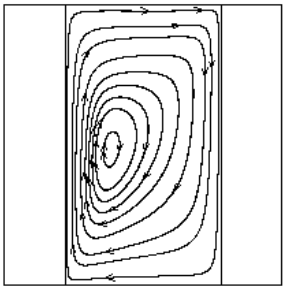

(c) Streamlines

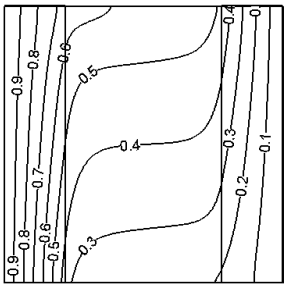

isotherms

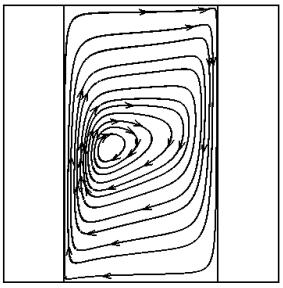

(d) Streamlines

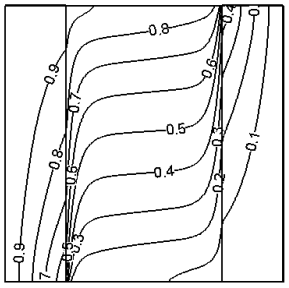

isotherms

Figure (3) Streamlines, isotherms lines for $Da=10^{-6}$, $Ra=1*10^{9}$, Pr=1.0, Kr=1 at (a),D=0.0, (b)D=0.2, (c) D=0.4, and at (d) Kr=10,D=0.4

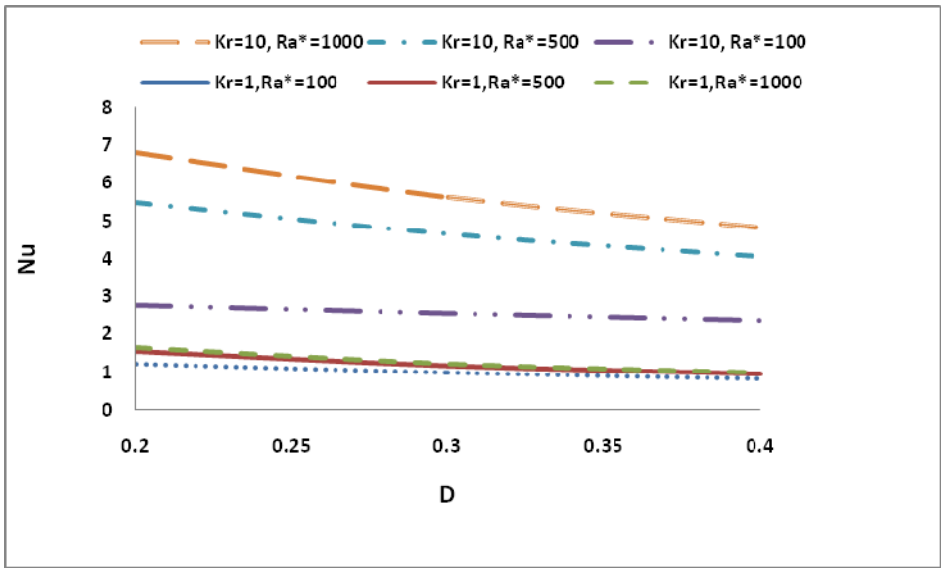

Figure (4) Variation of average Nusselt number on the interface left wall porous with wall thickness at Da=10^{-7}, Pr=1.0

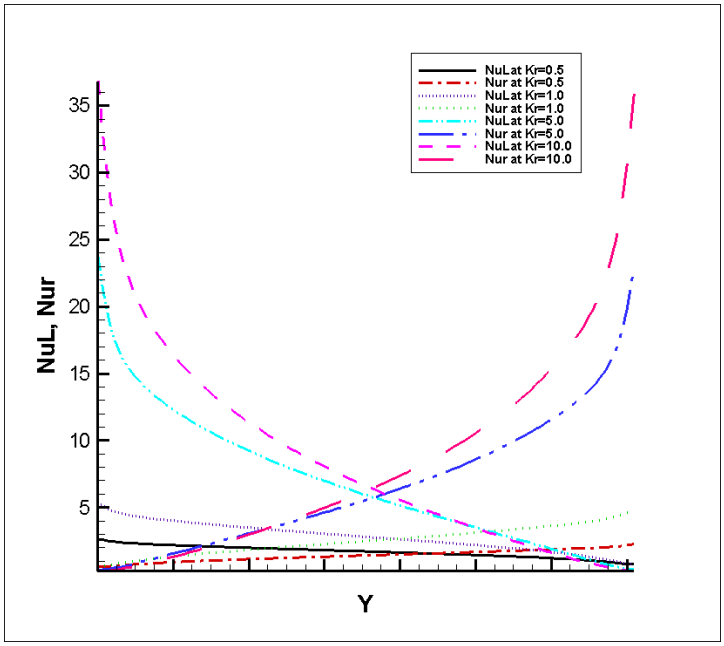

Figure (5) Variation of Left and right local Nusselt number on the vertical interface walls with thermal conductivity ratio for Da=10^{-6}, Ra=1*10^{9}, Pr=1.0, D=0.1

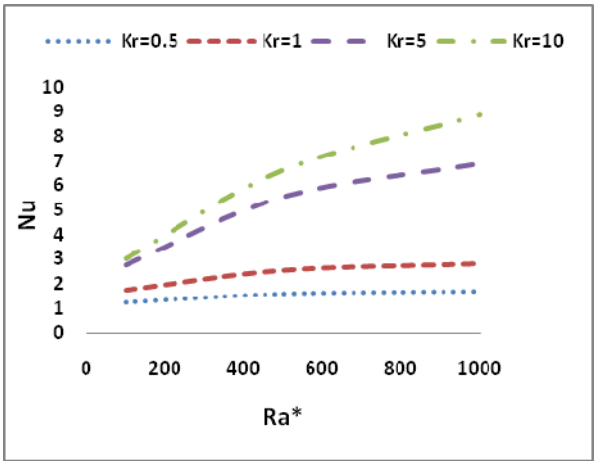

Figure (6) variation of Nusselt numbers with Ra* for Da=10^{-6}, Pr=1.0 and D=0.1